ISBN: 978-3-95450-191-5 doi:10.18429/JACoW-SRF2017-MOPB011

CEA CRYOMODULES DESIGN FOR SARAF PHASE 2

C. Madec, N. Bazin, R. Cubizolles, D. Chirpaz, P. Hardy, F. Leseigneur, T. Plaisant, J. Plouin, P. Bredy, R. Bruce, CEA, Saclay, France

Abstract

CEA is committed to delivering a Medium Energy Beam Transfer line and a SuperConducting Linac (SCL) for SARAF accelerator in order to accelerate 5mA beam of either proton from 1.3MeV to 35MeV or deuterons from 2.6 MeV to 40.1MeV. The SCL [1,2] consists in 4 cryomodules separated by warm section housing beam diagnostics. The first two identical cryomodules host 6 half-wave resonator (HWR) low beta (0.091) cavities 176 MHz. The two last identical cryomodules are equipped with 7 HWR high beta (0.181) cavities, 176 MHz. The beam is focused through solenoids located between cavities housing steering coils. A beam position monitor is placed upstream each solenoid. The warm section contains a beam profiler and a vacuum pump will be placed at the end of each cryomodule. The cryomodules and warm sections are being designed. These studies will be presented in this poster.

INTRODUCTION

The SARAF-Phase II cryomodule design [2] is based on CEA experience on designing QWR and HWR cryomodule (SPIRAL2 and IFMIF). Figure 1 presents the SARAF Phase 2 cryomodule and its main components.

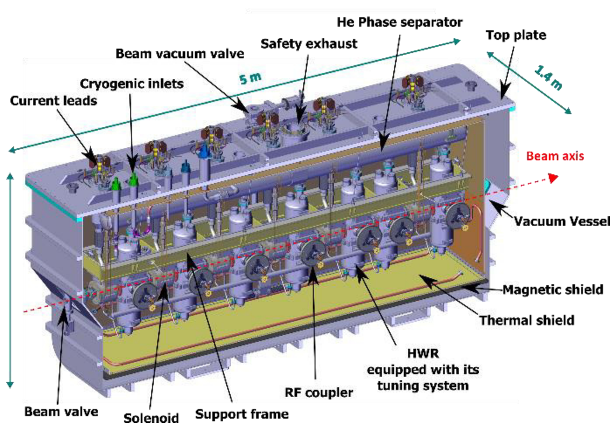

Figure 1 : SARAF phase 2 low beta cryomodule.

The infrastructures impose the lateral dimensions of the cryomodules since during the installation and maintenance, the cryomodules need to be moved freely in the beam corridor without disassembling any components of the accelerator line. Thus, the cavities have been placed vertically and the power coupler horizontally. In order to ease the assembly of the cryomodule, the cold mass will be hung on the top plate and top loaded into the vacuum vessel. The interfaces will be gathered on the top plate. Beam dynamics studies have determined the number of solenoids and cavities for the two types of cryomodules as well as the length of the string (cavities and solenoids) to 4.5 m for the low beta and 4.9 for the high beta. If the cavities performance are not reached in the first cryomodule, a free space for an optional cavity has been placed between the 5th and 6th cavity of the second low-beta cryomodule Figure 1. Moreover, the beam dynamic studies also impose a limitation on the cavity string misalignment at cold of +/- 2 mm. Hence, due to the impact on the cavity string alignment of the support frame, top plate and vacuum vessel, these components have been designed in order to ensure the alignment specifications and the results were presented in [3] together with the simulations and results on the top plate, support frame and vacuum vessel. Studies and simulations on the thermal and magnetic shield, phase separator, beam vacuum and assembly process were carried out. All those studies are presented in this contribution. Following simulations were performed with the finite elements software Cast3M.

THERMAL SHIELD

The thermal shield aims at reducing the radiative heat load from the room temperature parts of the cryomodule on the cold mass which is at liquid helium temperature. Indeed, the radiative heat flux between 300 K and 4 K is around 52 W/m² without a thermal intercept. With a thermal shield whose temperature is around 80 K, the value is reduced to 0.18 W/m² if no multi-layer insulation is installed on the 4 K parts. The thermal shield is also used to heat sink the components where one end is at room temperature and the other at liquid helium temperature, such as the RF power couplers, the current leads of the solenoid packages, the warm-cold transitions, etc. The heat loads on the Lβ and Hβ thermal shield are similar (respectively about 230 W and 220 W). Hence, the presented studies are based on the dimension of the Lβ thermal shield.

The simulations of the thermal shield aim at verifying the temperature of the thermal shield during cooling down and the mechanical deformation depending on the material (copper and aluminium).

Mechanical Design

The thermal shield is hung inside the vacuum vessel thanks to eight rods attached between the top part of the thermal shield and the top plate. These rods are made of titanium alloy for mechanical issues and in order to reduce the thermal losses, as the thermal conductivity is lower than the one of stainless steel. They are about 50 mm long. The deflection of top part of the thermal shield has to be under 5mm considering the space between the magnetic shield and the thermal shield covered by multi-layer insulator (about 25 mm between the magnetic shield and the thermal shield without the MLI) and the manufacturing and assembly errors. In order to ease the manufacturing of the shield made of plates, the same thickness for

ISBN: 978-3-95450-191-5 doi:10.18429/JACoW-SRF2017-MOPB011

the plates will be used. Thus, an estimation of the deformations of the top part versus the shield thickness has been carried out showing that a thickness of 5 mm ensures a deformation under 5 mm for aluminium and copper. Figure 2 presents the deformation of one fourth of the top part of the thermal shield with a thickness of 5 mm for different materials. The deformation of the top part is 3.5 mm for the copper and 1.6 mm for the aluminium.

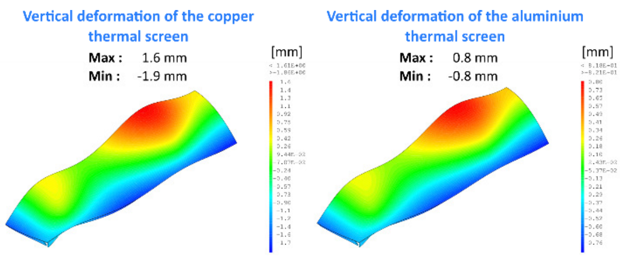

Figure 2 : Vertical deformations of a quarter of the shield top part depending on the material.

Figure 3 presents the Von Mises stress of the top part of the thermal shield for aluminium and for copper.

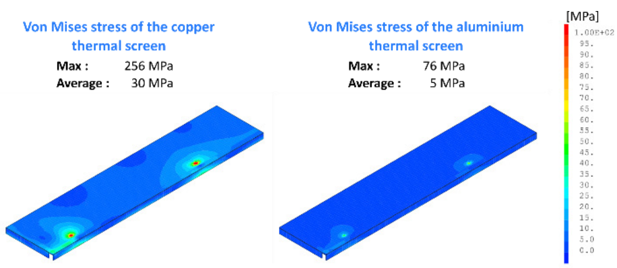

Figure 3 :Von Mises stress of a quarter of the shield top part depending on the material.

The high values of stress (red on Figure 3) correspond to the boundary conditions of the models, the supporting of the top part is made on points of the mesh. For the two materials, the average stress is acceptable. Thus, a thickness of 5 mm is taken for the following simulations.

Thermal Simulation

Knowing the thickness, an estimation of the cooling time was analytically performed showing that the requested cool down time (24H) could be reached taking into account the different type of heat loads using the copper, stainless steel and Titanium coefficient. To limit the radiation, the thermal shield is covered of 30 layers of multi-layer insulating and the heat flux is 3 W/m² at 60 K. Figure 4 presents the heat loads versus the temperature for the different contributions.

Then, simulations were performed in steady state for each type of material with the boundary conditions of the last step of the transient simulations. Figure 5 and Figure 6 present the temperature of the thermal shield made of aluminium and copper at the end cool down, when the shield temperature is stable. The maximum temperature is 70.9 K for a thermal shield made of Aluminium and 65.0 K for copper. In these figures, the thermal shield parts in red highlight a temperature over 70 K. The temperature of the thermal shield is relatively homogenous and does not present hot spot over 80 K. The maximum temperature is reached close to the cryogenic chimney corresponding to the safety chimney of the phase separator. However, the average temperature of the thermal shield is under 70K for every type of materials. The choice of the material for the thermal shield is not yet fixed. During call for tenders process, companies may propose either material.

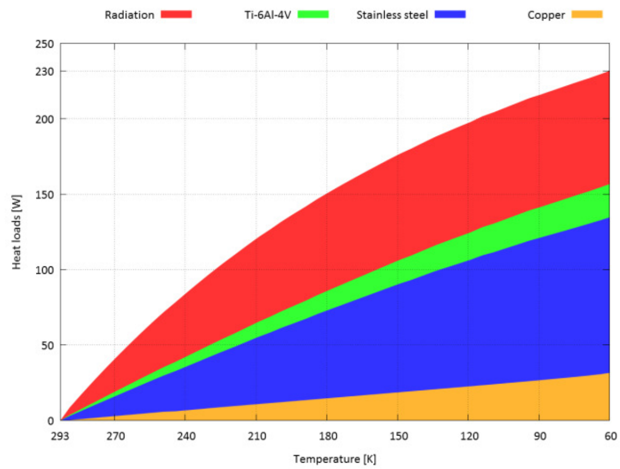

Figure 4 : Heat loads contributions depending on temperature.

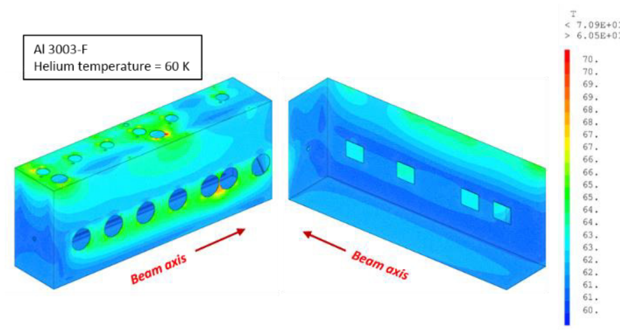

Figure 5 : Temperature of the thermal shield made of Al 3003-F (steady state).

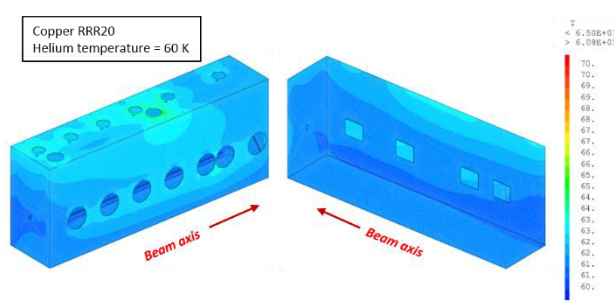

Figure 6 : Temperature of the thermal shield made of copper (steady state).

MAGNETIC SHIELD

In order to avoid trapping magnetic flux while cooling down through niobium transition, the superconducting cavity must be protected against the background magnetic field. Two basic variants are possible to reach the target value of 2µT around the half-wave resonator: the global

ISBN: 978-3-95450-191-5 doi:10.18429/JACoW-SRF2017-MOPB011

shield and the local shield. In the global shield, a high permeability nickel alloy mu-metal is installed on the inner surface of the vacuum vessel and operates at room temperature. In the local shield, a cold service special mu-metal (CRYOPERM or CRYOPHY) is place locally around the cavity.

Due to its simplicity in design, manufacturing and assembly, it has been decided to use a global magnetic shield. Though, room has been reserved around the cavity to accommodate a local shield if deemed necessary during prototype measurements. For Spiral 2 and the IFMIF-EVEDA cryomodules, the magnetic shield is fixed on the inner surface of the vacuum vessel. Because of manufacturing defects of the vacuum vessel, the assembly of the shield inside the vessel was difficult for the Spiral 2 cryomodules, and for the IFMIF-EVEDA one, it has been decided not to fix every panels of the magnetic shield on the vessel inner surface, but to have a "floating" shield between the vacuum vessel and the thermal shield. For the simulations, an external uniform magnetic field of 50 µT corresponding to the earth magnetic field is applied successively in the 3 directions X, Y and Z. Figure 7 present the results of the simulations on the plane (X, 0, Z): when the magnetic field is over 2 µT the colour is white. As the magnetic field close to the torus of the superconducting cavities is the most critical, the field is also calculated along four lines as shown in Figure 9.

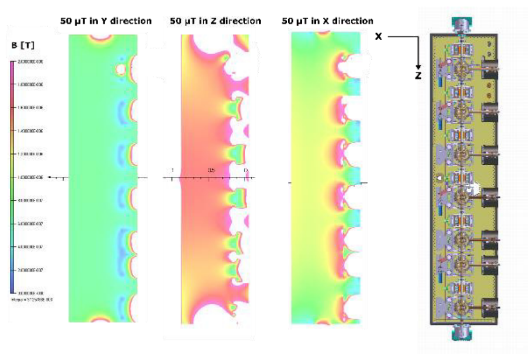

Figure 7: Magnetic field on the plane (X, 0, Z) with an external field of 50 µT on the Y, Z and X direction.

The magnetic field is under 2 µT at the cavity string in the two planes of the cryomodule for an external magnetic field in the X or Y direction. However, the shielding close to the interface of the power couplers and the vacuum vessel could be more efficient, as in the Z direction, the field is over the 2 µT in the center of the last cavity of the cryomodule in the planes (X, 0, Z) and (O, Y, Z). This is due to the wide opening in the magnetic shield needed for the interface flange of the warm – cold transition.

To conclude, a 2 mm thick magnetic shield is sufficient to protect the half wave resonator against the earth's magnetic field. However, the shielding around the couplers ports and the ports for the warm – cold transitions has to be studied more in details.

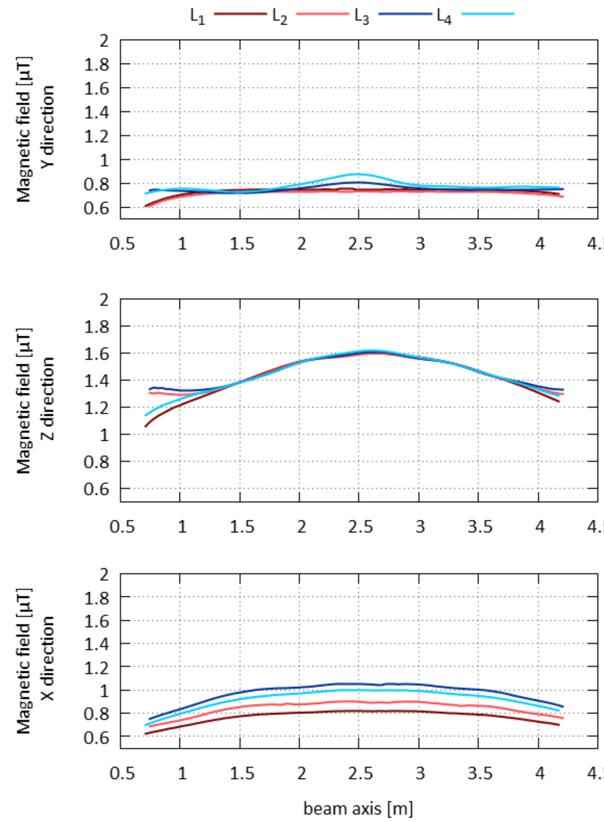

Figure 8 : Magnetic field on HPR port lines for the different external field direction.

PHASE SEPARATOR

Cavities or solenoids are connected to the phase separator thanks to two bellows to compensate heat shrinking issues as depicted in Figure 9. The stroke has to cope with the differential vertical, longitudinal and transversal displacements of the cavity string and the phase separator, but also to compensate the manufacturing defects of the components. The vertical displacement of the phase separator is set to 1.5 mm and the deflection of the main phase separator close to the helium outlet under 0.5 mm in order to lower the stress in the bellows. The simulations were performed in a pessimist case where the maximal internal pressure is reached (2 bars absolute inside the phase separator, vacuum outside) and the fixed flange of the safety chimney is at room temperature. The simulations will verify the deflection of the phase separator to be under 0.5 mm, the maximal vertical displacement of the phase separator to be under 1.5 mm, the maximum stress to be under the yield stress of the material, taking into account a safety margin.

As the phase separator is hung by its safety chimney flange, the chimney tube has to support the weight of the whole phase separator filed with helium. For a 2 mm thick and 150 mm diameter tube, the average stress is 2.1 MPa for attractive force of 2000 N (estimated weight of the separator). In order to standardize the thickness of the raw material for the manufacturing of the component, the Roak formula has been used to check that a 2mm thick

ISBN: 978-3-95450-191-5 doi:10.18429/JACoW-SRF2017-MOPB011

and 4 meters long tube stands atmospheric pressure with vacuum inside. Then, simulations were carried out on three different configuration (Figure 10).

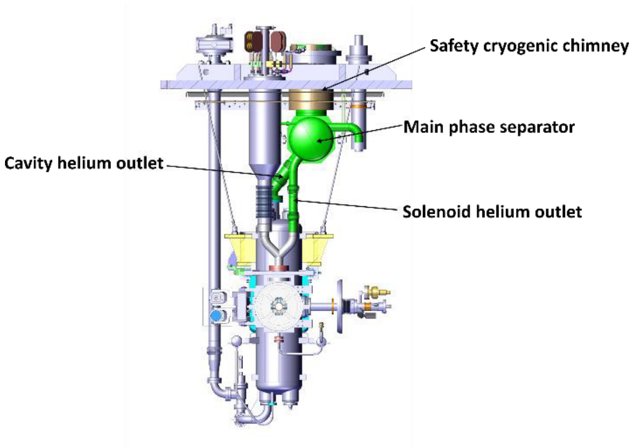

Figure 9: Solenoid and cavity helium outlet.

Results showed that the junction of the safety chimney and the main body of the phase separator has to be reinforced in order to get required deformation and stress. It could be done by using a thicker tube at the junction or made this one from one block. The latest presents advantages for the manufacturing and the welding of the different tubes. Moreover, the corners of the block can be machined in order to decrease its weight and to save space.

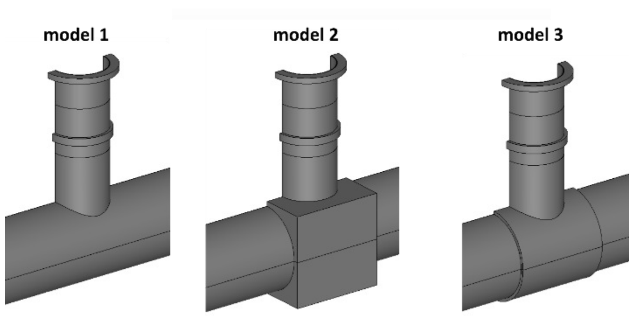

Figure 10: Models used for the simulations of the main phase separator.

CONCLUSION

The preliminary design has been validated by a review. The detailed design phase is going on for the cryomodules. Tooling will be developed and tests stand are being built. Components (cavities and solenoids) are being procured.

REFERENCES

[1] C. Madec *et al.*, "Design of the superconducting linac for SARAF", in *Proc. SRF'15*, Whistler, BC, Canada, Sep. 2015, paper MOPB063, pp. 250-254.

[2] N. Pichoff *et al.*, "The SARAF-LINAC project status", in *Proc. IPAC'17*, Copenhagen, Denmark, May 2017, paper TUPVA052, pp. 2194-2196.

[3] R. Cubizolles *et al.*, "CEA preliminary design of the cryomodules for SARAF Phase II superconducting LINAC", *in Proc. IPAC'17*, Copenhagen, Denmark, May 2017, paper MOPVA042.